*Anal. Chem.* **2005,** *77,* 7172−7182

# Using Comprehensive Two-Dimensional Gas Chromatography Retention Indices To Estimate Environmental Partitioning Properties for a Complete Set of Diesel Fuel Hydrocarbons

**J. Samuel Arey,* Robert K. Nelson, Li Xu, and Christopher M. Reddy**

*Department of Marine Chemistry and Geochemistry, Woods Hole Oceanographic Institution, Woods Hole, Massachusetts 02543*

**Comprehensive two-dimensional gas chromatography (GC×GC) provides nearly complete composition data for some complex mixtures such as petroleum hydrocarbons. However, the potential wealth of physical property information contained in the corresponding two-dimensional chromatograms is largely untapped. We developed a simple but robust method to estimate GC×GC retention indices for diesel-range hydrocarbons. By exploiting *n*-alkanes as reference solutes in both dimensions, calculated retention indices were insensitive to uncertainty in the enthalpy of gas−stationary-phase transfer for a suite of representative diesel components. We used the resulting two-dimensional retention indices to estimate the liquid vapor pressures, aqueous solubilities, air−water partition coefficients, octanol−water partition coefficients, and vaporization enthalpies of a nearly complete set of diesel fuel hydrocarbons. Partitioning properties were typically estimated within a factor of 2; this is not as accurate as some previous estimation or measurement methods. However, these relationships may allow powerful and incisive analysis of phase-transfer processes affecting petroleum hydrocarbon mixtures in the environment. For example, GC×GC retention data might be used to quantitatively deconvolve the effects of water washing and evaporation on environmentally released diesel fuels.**

Unlike more conventional separation methods, comprehensive two-dimensional gas chromatography (GC×GC) has dramatically resolved the chemical compositions of complex organic mixtures such as plant extracts,[1] cigarette smoke,[2] and weathered petroleum[3] since its inception[4] 14 years ago. A sample mixture is separated using two columns that are joined serially by a cryogenic modulator. Mixture components eluting from the first "dimension" (usually a nonpolar column) are trapped by the modulator and then fully transferred to the second dimension (usually a semipolar column) at discrete time intervals; hence the analysis is comprehensive. Transport through the second column is fast compared to retention in the first column; consequently the resolving effects and signal-to-noise ratios of the two dimensions are approximately multiplicative.[5] GC×GC has successfully separated thousands of peaks in mixtures where traditional one-dimensional chromatography differentiated fewer than 100 peaks.[6] Thus far, GC×GC studies have focused primarily on enhancing the resolving power of the instrument and increasing the range of mixture types that can be separated.[5,7,8]

As Reddy et al.[9] observed qualitatively, the wealth of mixture composition information derived from GC×GC could be further exploited by relating retention data to the partitioning properties of analyzed mixture components. Reddy et al. used GC×GC to analyze the residual hydrocarbon mixture that persisted in marsh sediments of Wild Harbor, MA, 30 years after this coastal wetland was contaminated by an uncontrolled release of a diesel oil from the barge, *Florida*. By comparing a GC×GC chromatogram of the residual hydrocarbon contamination with that of a neat diesel oil, they found that small, aromatic hydrocarbon components had been preferentially removed from the spilled oil. Additional analyses of artificially evaporated diesel oil samples revealed that volatilization systematically removed compounds along the first dimension of the GC×GC chromatogram. The anticipated cumulative "signatures" of volatilization, biodegradation, and phototransformations did not adequately explain the weathering trends observed in the GC×GC data of the residuum of the spilled oil. Reasoning that small, aromatic hydrocarbon compounds probably constituted the most water-soluble components of the *Florida* diesel oil, Reddy et al. suggested that these had been removed from the spilled oil more by water washing than by evaporation. Precisely disentangling these phase-transfer processes and evaluating their quantitative impact on the mixture was impossible by

* Corresponding author: (e-mail) arey@alum.mit.edu; (phone) +41 21 693 0323; (fax) +41 21 693 0320.

(1) Dimandja, J. M. D.; Stanfill, S. B.; Grainger, J.; Patterson, D. G. *J. High Resolut. Chromatogr.* **2000**, *23*, 208−214.
(2) Dalluge, J.; van Stee, L. L. P.; Xu, X. B.; Williams, J.; Beens, J.; Vreuls, R. J. J.; Brinkman, U. A. T. *J. Chromatogr., A* **2002**, *974*, 169−184.
(3) Frysinger, G. S.; Gaines, R. B.; Xu, L.; Reddy, C. M. *Environ. Sci. Technol.* **2003**, *37*, 1653−1662.
(4) Liu, Z. Y.; Phillips, J. B. *J. Chromatogr. Sci.* **1991**, *29*, 227−231.
(5) Giddings, J. C. *J. Chromatogr., A* **1995**, *703*, 3−15.
(6) Venkatramani, C. J.; Phillips, J. B. *J. Microcolumn Sep.* **1993**, *5*, 511−516.
(7) Grainger, J.; McClure, P. C.; Liu, Z. Y.; Botero, B.; Sirimanne, S.; Patterson, D. G.; Sewer, M.; Gillyard, C.; Kimata, K.; Hosoya, K.; Araki, T.; Tanaka, N.; Terabe, S. *Chemosphere* **1996**, *32*, 13−23.
(8) Gaines, R. B.; Frysinger, G. S. *J. Sep. Sci.* **2004**, *27*, 380−388.
(9) Reddy, C. M.; Eglinton, T. I.; Hounshell, A.; White, H. K.; Xu, L.; Gaines, R. B.; Frysinger, G. S. *Environ. Sci. Technol.* **2002**, *36*, 4754−4760.



10.1021/ac051051n CCC: $30.25 
Published on Web 10/14/2005

visual inspection. However, if the measured GC×GC retention times of hydrocarbon analytes could be robustly related to their environmental partitioning properties, one could quantify the detailed compositional changes of a petroleum mixture resulting from evaporation and water washing in the environment. Effectively differentiating the effects of these processes on hydrocarbon mixtures remains a standing challenge to the environmental chemistry community.

Previous work has shown that GC retention indices of some organic compounds may be used to estimate their equilibrium partitioning properties, $P$, in various liquid−liquid or vapor−liquid systems. Following Bidleman,[10] it has become accepted that hypothetical liquid vapor pressures of many organic compounds may be estimated using GC retention factors or retention indices[11−13] (see Letcher and Naicker[14] for a review). Additional work[15−17] has shown that octanol−water partition coefficients and liquid aqueous solubilities of nonpolar solutes also correlate with gas chromatography retention data, by the relationship

$$\log P_{xy,i}(25\ ^\circ\mathrm{C}) = a_{xy}I_{s,i} + b_{xy} \qquad (1)$$

where $P_{xy,i}$ is the partitioning property (liquid vapor pressure, octanol−water partition coefficient, or liquid aqueous solubility) of solute $i$ at 25 °C, $I_{s,i}$ is a retention index of solute $i$ on a nonpolar stationary phase $s$, and $a_{xy}$ and $b_{xy}$ are fitted constants for a particular solute family in partitioning system $x$−$y$. In these studies, the log $P_{xy,i}$ values within a solute family varied in only one aspect of the solute−solvent interaction: namely, the solute size dependence of the partial molar excess free energy of solute transfer from phase $y$ to phase $x$ ($\Delta G_{xy,i}$). Likewise, the $I_{s,i}$ values effectively measured a $\Delta G_{sg,i}$ (partial molar excess free energy of gas−stationary-phase transfer) scale which, within a solute family, explored variability related to solute size. The corresponding solute−solvent interactions include the solvent cavitation energy and some van der Waals information, but hydrogen-bonding and strong polar interactions are not generally included.[18,19] Hence it must be emphasized that conventional linear free energy relationships (LFERs) such as eq 1 are robust only when applied to individual solute families.[18−21]

GC×GC could add an extra dimension of information to eq 1 and thereby offer a powerful approach for simultaneously estimating the solvation properties of hundreds or thousands of solutes found in complex mixtures. Abraham and co-workers have shown that no more than five dimensions of solute−solvent interaction information are required to accurately explain the partitioning properties of thousands of different organic solutes in hundreds of different solvents.[22,23] These governing solvation parameters correspond to five physical features of the solute: size, excess polarizability, polarity, hydrogen bond-accepting capacity, and hydrogen bond-donating capacity.[23] Using conventional one-dimensional, single-stationary-phase gas chromatography, several separate experiments are normally required to adequately characterize all of these descriptors for a single solute.[22,23] Or, conventional gas chromatography may be used to interrelate log $P$ values within a solute family along one dimension of a solute partitioning property, vis-à-vis LFERs such as eq 1. By contrast, GC×GC explores two dimensions of information about solute−solvent physical interactions for hundreds or thousands of solutes in a mixture with a single measurement. Consequently, GC×GC retention time data might be used to estimate solute partitioning properties for systems in which solute−solvent interactions reflect primarily only two dimensions of physical interaction information.

Our main goal was to establish whether GC×GC retention data could predict partitioning properties of diesel fuel hydrocarbon solutes for a range of other liquid−liquid and vapor−liquid systems. For hydrocarbon solutes in polar and nonpolar solvents, we suspected that solute size[24] and van der Waals (solute electrostatic[25] plus solute polarization[26]) interactions with the solvent would control the log $P$ more significantly than hydrogen bonding. We hypothesized that GC×GC retention indices would accurately convey information about both solute size and solute polarity/polarizability and therefore might be used to estimate the log $P$ values of diesel fuel solutes in other partitioning systems, using the LFER

$$\log P_{xy,i}(25\ ^\circ\mathrm{C}) = a_{xy}I_{1,i} + b_{xy}I_{2,i} + c_{xy} \qquad (2)$$

where $I_{1,i}$ is the GC×GC first dimension retention index of solute $i$, $I_{2,i}$ is the GC×GC second dimension retention index of solute $i$, and $a_{xy}$, $b_{xy}$, and $c_{xy}$ are fitted constants that are specific to partitioning system $x$−$y$. To implement eq 2, it was first necessary to convert raw retention time data into retention indices in both the first and second dimensions. Constructing accurate retention indices from GC×GC retention data is still an emerging topic of investigation,[27−29] and we explain the development of these steps in Theoretical Applications. If eq 2 is successful, scientists could use GC×GC to analyze phase-transfer processes affecting complex mixtures. A secondary goal was to evaluate the basis for solute−solvent interactions of both dimensions of the GC×GC retention space. This would directly reveal what types of "sample dimensions", or linearly independent sample properties, one could expect to resolve using a particular GC×GC setup.


(10) Bidleman, T. F. *Anal. Chem.* **1984**, *56*, 2490−2496.
(11) Eitzer, B. D.; Hites, R. A. *Environ. Sci. Technol.* **1988**, *22*, 1362−1364.
(12) Hinckley, D. A.; Bidleman, T. F.; Foreman, W. T.; Tuschall, J. R. *J. Chem. Eng. Data* **1990**, *35*, 232−237.
(13) Fischer, R. C.; Wittlinger, R.; Ballschmiter, K. *Fresenius J. Anal. Chem.* **1992**, *342*, 421−425.
(14) Letcher, T. M.; Naicker, P. K. *J. Chromatogr., A* **2004**, *1037*, 107−114.
(15) Miller, M. M.; Ghodbane, S.; Wasik, S. P.; Tewari, Y. B.; Martire, D. E. *J. Chem. Eng. Data* **1984**, *29*, 184−190.
(16) Hawker, D. W.; Connell, D. W. *Environ. Sci. Technol.* **1988**, *22*, 382−387.
(17) Hackenberg, R.; Schutz, A.; Ballschmiter, K. *Environ. Sci. Technol.* **2003**, *37*, 2274−2279.
(18) Ballschmiter, K.; Ellinger, S.; Hackenberg, R. *Environ. Sci. Technol.* **2004**, *38*, 2288−2288.
(19) Fenner, K.; Roth, C.; Goss, K. U.; Schwarzenbach, R. P. *Environ. Sci. Technol.* **2004**, *38*, 2286−2287.
(20) Goss, K. U.; Schwarzenbach, R. P. *Environ. Sci. Technol.* **2001**, *35*, 1−9.
(21) Schwarzenbach, R. P.; Gschwend, P. M.; Imboden, D. M. *Environmental Organic Chemistry*, 2nd ed.; John Wiley & Sons: New York, 2003.
(22) Abraham, M. H.; Poole, C. F.; Poole, S. K. *J. Chromatogr., A* **1999**, *842*, 79−114.
(23) Abraham, M. H.; Ibrahim, A.; Zissimos, A. M. *J. Chromatogr., A* **2004**, *1037*, 29−47.
(24) Abraham, M. H.; McGowan, J. C. *Chromatographia* **1987**, *23*, 243−246.
(25) Abraham, M. H.; Whiting, G. S. *J. Chromatogr.* **1991**, *587*, 213−228.
(26) Abraham, M. H.; Whiting, G. S.; Doherty, R. M.; Shuely, W. J. *J. Chem. Soc., Perkin Trans. 2* **1990**, 1451−1460.
(27) Western, R. J.; Marriott, P. J. *J. Sep. Sci.* **2002**, *25*, 832−838.
(28) Western, R. J.; Marriott, P. J. *J. Chromatogr., A* **2003**, *1019*, 3−14.
(29) Marriott, P. J.; Massil, T.; Hugel, H. *J. Sep. Sci.* **2004**, *27*, 1273−1284.

## LABORATORY ANALYSIS

**GC×GC Method A.** To determine the retention indices of diesel-range hydrocarbons by GC×GC, a mixture of several components was prepared and analyzed. Diesel fuel from the spill of the barge *Bouchard 65*, which occurred in October 1974 in Buzzards Bay, MA,[30] was amended with additional parent and alkylated polycyclic aromatic hydrocarbons (PAHs), linear alkylbenzenes (LABs), and linear alkylcyclohexanes (LACs). Most of these added standard compounds were already present in the original diesel fuel; the amendments simply ensured accurate detection of several homologous sets of representative diesel hydrocarbons. The standards were purchased from the National Institute of Standards and Technology (Gaithersburg, MD), Chiron (Trondheim, Norway), and Sigma-Aldrich (St. Louis, MO). The mixture was analyzed on a GC×GC system that employed an Agilent 6890 gas chromatograph configured with a 7683 series split/splitless autoinjector, two capillary gas chromatography columns, a model KT-CLM-ZOE02 loop jet modulator (Zoex Corporation, Lincoln, NB), and a flame ionization detector. The sample was injected in splitless mode and the purge vent was opened at 2.0 min. The inlet temperature was 280 °C. The first-dimension column and the loop jet modulator reside in the main oven of the Agilent 6890 gas chromatograph. A smaller oven houses the second-dimension column. With this configuration, the temperature profiles of the first-dimension column, thermal modulator (hot jet), and the second-dimension column can be independently programmed. The first-dimension column was a nonpolar 100% dimethyl polysiloxane phase (Restek Rtx-1 Crossbond, 7-m length, 0.10-mm-inner diameter (i.d.), 0.4-$\mu$m film thickness) that was programmed to remain isothermal at 35 °C for 5 min and then ramped from 35 to 180 °C at 0.66 °C min$^{-1}$. The modulation loop was a deactivated fused-silica column (1.5-m length, 0.10-mm i.d.) that joined the end of the first-dimension column to the beginning of the second-dimension column. The thermal modulator (hot jet) was heated to 100 °C above the temperature in the main oven to ensure that all trapped compounds were thoroughly and rapidly desorbed[8] from the cold spot. The hot jet pulse frequency was 12.5 s (0.08 Hz), and the pulse duration was 300 ms. The cold jet gas was dry $N_2$ chilled with liquid Ar and had a flow rate of 3.5 L min$^{-1}$. Second-dimension separations were performed on a 50% phenyl polysilphenylene−siloxane column (SGE BPX50, 0.82-m length, 0.10-mm i.d., 0.1-$\mu$m film thickness) that was programmed to remain isothermal at 60 °C for 5 min and then ramped from 60 to 241 °C at 0.79 °C min$^{-1}$. The carrier gas was $H_2$ at a constant flow rate of 1.6 mL min$^{-1}$. The flame ionization detector (FID) signal was sampled at 100 Hz. Sample dilutions confirmed that the injected amount did not affect retention times of the solutes; that is, the infinite dilution approximation was valid for the GC×GC stationary phases at the applied injection loading range. Using a program and setup very similar to that described here, retention times of individual solute peaks were highly reproducible in seven duplicate sample runs. In these experiments, the peak positions of both pristane (a nonpolar hydrocarbon) and phenanthrene (a polar hydrocarbon) were found to have no measurable variability in the first dimension (i.e., deviations were smaller than the modulation period of 12.5 s) and a standard deviation of 0.01−0.02 s in the second dimension.

The holdup time of the second-dimension column was measured by injecting ethane and propane into the GC×GC at the initial temperature. These gases were partly trapped by the cold jet modulator and were assumed unretained in the heated sections of both GC×GC columns. To calculate the second-dimension holdup time ($t_2^m$), we needed to account for the length of deactivated column joining the cold trap and the second-dimension activated column. In the second dimension, ethane and propane peaks were found to elute simultaneously with the (also modulated) slight column bleed originating from the first column. Therefore we concluded that the delay time between engagement of the hot jet and detection of the eluting column bleed corresponded to the gas-phase transport time in the deactivated loop plus semipolar second column. The breakthrough front of the modulated column bleed was used to calculate $t_2^m$ throughout the entire GC×GC run.

**GC×GC Method B.** It was necessary to confirm that the retention index estimates and resulting physical property estimates were not spuriously dependent on the particular settings of the original analysis method (GC×GC method A). In a separate GC×GC run, we analyzed the amended diesel fuel mixture using the same instrumentation and approach as described in method A, but we modified several instrument settings. The "primary" parameters that directly affect solute retention times and chromatographic separation were changed as follows: the first-dimension activated column length was 6.5 m; the second-dimension activated column length was 0.60 m; the total deactivated modulation loop length was 1.445 m; the first dimension oven was programmed to remain isothermal at 37 °C for the first 5 min and then was ramped from 37 to 307 °C at 1.5 °C min$^{-1}$; the second dimension was isothermal at 70 °C for 5 min and then was ramped from 70 to 340 °C at 1.5 °C min$^{-1}$; and the $H_2$ carrier flow gas rate was 1.5 mL min$^{-1}$. Some "secondary" settings also differed from method A: the purge vent was opened at 2.5 min; the inlet temperature was 300 °C; and the cold jet gas ($N_2$) had a flow rate of 4.0 L min$^{-1}$.

**Conventional One-Dimensional GC.** To compare the retention indices estimated from GC×GC retention data against measured Kovàts values, we analyzed select compounds by conventional one-dimension gas chromatography on an Agilent 6890 gas chromatograph with an FID. The retention times of alkanes, LACs, LABs, and PAHs at 120 °C were measured on a 100% dimethylpolysiloxane column (Restek Rtx-1 Crossbond, 6-m length, 0.10-mm i.d., 0.4-$\mu$m film thickness) and, in a separate experiment, on a 50% phenylpolysilphenylene−siloxane column (SGE BPX50, 6-m length, 0.10-mm i.d., 0.1-$\mu$m film thickness). At least six repeated retention time measurements were taken for each solute. Holdup times were measured using ethane injections.

## THEORETICAL CONSIDERATIONS

To apply eq 2, we converted raw GC×GC retention time data into corresponding retention index estimates; this method is described in the first two sections. Evaluation of eq 2 using measured partitioning data for hydrocarbon solutes is reported in the results.

**Retention Index of the GC×GC First Dimension.** Since *n*-alkanes eluted as a regular series in the GC×GC first dimension,

(30) Reddy, C. M. *Oceanus* **2004**, *43*, 50−55.

the retention index values of all hydrocarbon solutes were interpolated to *n*-alkane carbon number ($N_c$) using the method of piecewise cubic splines.[31] This procedure resulted in the commonly used linear temperature retention index,[32] referred to as $I_{1,i}$. The index was expressed in "index units" (iu), defined by $I_{1,n-\text{alkane}} = 100\ N_c$. $I_{1,i}$ only approximates the Kováts index;[33,34] that is, $I_{1,i}$ is not a rigorous $\Delta G_{1g,i}$ scale across hydrocarbon solutes. We may expect a small but systematic departure of $I_{1,i}$ from a Kováts index with decreasing solute saturation,[35] because the heat capacity change upon vaporization ($\Delta C_p$) for a flexible hydrocarbon solute (e.g., alkane) typically exceeds that of a rigid hydrocarbon solute (e.g., PAH) of similar volatility.[34,36,37] To evaluate the accuracy of the linear temperature index, we compared $I_{1,i}$ values for several LACs, LABs, and PAHs to the corresponding Kováts indices ($I'_{1,i}$) measured using a conventional GC with an Rtx-1 phase at 120 °C (see Laboratory Analysis).

**Retention Index of the GC×GC Second Dimension.** To generate a physically meaningful second-dimension retention index, measured second-dimension retention times were converted into ln $K_{2g,i}(T_o)$ estimates, where $K_{2g,i}(T_o)$ is the stationary-phase−gas-phase partition coefficient of solute $i$ at a reference temperature, $T_o$ (we chose $T_o = 120$ °C). In the GC×GC second dimension, solute elution occurs within seconds and therefore transport is approximately isothermal. Assuming negligible adsorption to the gas−stationary-phase interface or column wall[38] and assuming dilute solution conditions in the stationary phase,[39,40] the second-dimension stationary-phase−gas-phase equilibrium partition coefficient, $K_{2g,i}(T)$, is related to the second-dimension isothermal retention time, $t^r_{2,i}(T)$, through[39]

$$K_{2g,i}(T) = \beta_2\left(\frac{t^r_{2,i}(T)}{t^m_2} - 1\right) \tag{3}$$

where $T$ is second-dimension temperature, $\beta_2$ is the second-dimension mobile-phase volume to stationary-phase volume ratio, and $t^m_2$ is the second-dimension gas holdup time. Equation 3 assumes equilibrium partitioning into the stationary phase, and while this supposition is common in chromatography, often it is not rigorously correct.[39] Therefore, in the following treatment, the apparent chromatographic "thermodynamic" terms were considered as an internally consistent set of near-equilibrium properties. The second-dimension column temperature was slowly ramped (e.g., 0.79 °C min$^{-1}$ using GC×GC method A) over the course of solute elution from the first dimension; consequently, solutes that eluted at different times from the first dimension experienced different temperature conditions (ranging from 55 to 340 °C) in the second dimension. Therefore some assumptions or information about the temperature dependence of $K_{2g,i}(T)$ were required to arrive at estimates of $K_{2g,i}$ ($T_o = 120$ °C). $K_{2g,i}(T)$ may be expressed in terms of the partial molar excess energy of solute transfer from the gas phase to the stationary phase, $\Delta G_{2g,i}$, by[21,41]

$$\ln K_{2g,i}(T) = -\frac{\Delta G_{2g,i}(T)}{RT} - \ln\left(\frac{\rho_g}{\rho_2}\right) \tag{4}$$

where $R$ is the molar gas constant (8.314 J mol$^{-1}$ K$^{-1}$) and $\rho_2$ and $\rho_g$ are the total molar concentrations of the second-dimension stationary phase and the gas phase, respectively. Employing the Gibbs−Helmholtz relation,[41] we integrated eq 4 from $T_o$ to $T$ to find

$$\ln K_{2g,i}(T) - \ln K_{2g,i}(T_o) = -\frac{\Delta H_{2g,i}}{R}\left(\frac{1}{T} - \frac{1}{T_o}\right) + \ln\left(\frac{T}{T_o}\right) \tag{5}$$

where $\Delta H_{2g,i}$ is the partial molar excess enthalpy of gas-phase−stationary-phase transfer of the solute, $\rho_2$ was assumed independent of $T$, and $\rho_g$ was treated using the ideal gas law. $\Delta H_{2g,i}$ was assumed constant with respect to $T$; in other words, heat capacity effects were ignored.

It was desirable to formulate the second-dimension retention index in a way that was not highly sensitive to uncertainty in $\Delta H_{2g,i}$ or the need for explicit heat capacity information. Western and Marriott[28] estimated GC×GC second-dimension retention indices by using $\Delta H_{2g,i}$ to extrapolate ln $K_{2g,i}(T_o)$ from ln $K_{2g,i}(T)$, via an expression similar to eq 5. These authors acknowledged the important disadvantages that accurate measurements of $\Delta H_{2g,i}$ were difficult and data intensive, and the resulting extrapolated retention index values were sensitive to uncertainty in this term. Additionally, we considered it practical to exploit *n*-alkanes as reference solutes, since these compounds eluted along the entire temperature range of the second dimension and have well-established physical−chemical properties. Proceeding from these criteria, we used eq 5 to express the difference between the ln $K_{2g,i}(T)$ of solute $i$ and that of a hypothetical *n*-alkane solute (*) eluting at the same temperature $T$ as solute $i$, as

$$\ln K_{2g,i}(T) - \ln K^*_{2g,i}(T) = \ln K_{2g,i}(T_o) - \ln K^*_{2g,i}(T_o) - \frac{(\Delta H_{2g,i} - \Delta H^*_{2g,i})}{R}\left(\frac{1}{T} - \frac{1}{T_o}\right) \tag{6}$$

We anticipated that the temperature correction term in eq 6 would be small relative to the quantity of interest, ln $K_{2g,i}(T_o)$, and that this might allow a simple approximation for $\Delta H_{2g,i}$. Based on the finding of Goss and Schwarzenbach that vaporization enthalpy is closely correlated ($r^2 = 0.99$) with liquid vapor pressure at 25 °C across 195 different organic compounds,[42] we assumed


(31) Halang, W. A.; Langlais, R.; Kugler, E. *Anal. Chem.* **1978**, *50*, 1829−1832.
(32) van den Dool, H.; Kratz, P. D. *J. Chromatogr.* **1963**, *11*, 463−471.
(33) Curvers, J.; Rijks, J.; Cramers, C.; Knauss, K.; Larson, P. *J. High Resolut. Chromatogr. Chromatogr. Commun.* **1985**, *8*, 607−610.
(34) Gonzalez, F. R.; Nardillo, A. M. *J. Chromatogr., A* **1999**, *842*, 29−49.
(35) Lai, W. C.; Song, C. S. *Fuel* **1995**, *74*, 1436−1451.
(36) Mishra, D. S.; Yalkowsky, S. H. *Ind. Eng. Chem. Res.* **1991**, *30*, 1609−1612.
(37) Myrdal, P. B.; Yalkowsky, S. H. *Ind. Eng. Chem. Res.* **1997**, *36*, 2494−2499.
(38) Kersten, B. R.; Poole, S. K.; Poole, C. F. *J. Chromatogr.* **1989**, *468*, 235−260.
(39) Giddings, J. C. *Dynamics of Chromatography*; Marcel Dekker: New York, 1965.
(40) Gonzalez, F. R. *J. Chromatogr., A* **2004**, *1037*, 233−253.
(41) Tester, J. W.; Modell, M. *Thermodynamics and Its Applications*, 3rd ed.; Prentice Hall: Upper Saddle River, NJ, 1997.
(42) Goss, K. U.; Schwarzenbach, R. P. *Environ. Sci. Technol.* **1999**, *33*, 3390−3393.

$$\Delta H_{2g,i}(\text{J/mol}) \approx a \ln K_{2g,i}(T_o) + b \quad (7)$$

for diesel hydrocarbons on a semipolar stationary phase at $T_o$ = 120 °C. Using eq 7 to describe both $\Delta H_{2g,i}$ and $\Delta H^*_{2g,i}$ in eq 6, rearranging and solving for $\ln K_{2g,i}(T_o)$ led to

$$\ln K_{2g,i}(T_o) = \ln K^*_{2g,i}(T_o) + \frac{1}{\left(1 - \frac{a}{R}\left(\frac{1}{T} - \frac{1}{T_o}\right)\right)} \ln\left(\frac{K_{2g,i}(T)}{K^*_{2g,i}(T)}\right) \quad (8)$$

The right-hand side terms in eq 8 were determined as follows. The $K_{2g,i}(T)$ value of solute $i$ was calculated from the measured second-dimension retention time, $t^r_{2,i}$, using eq 3. $K^*_{2g,i}(T)$ was also calculated from eq 3, based on the second-dimension retention time of a hypothetical *n*-alkane, $t^r_{2,i}*$, eluting at the same $T$ as solute $i$. We interpolated $t^r_{2,i}*$ from the measured $t^r_{2,i}$ values of nearby *n*-alkanes using the method of cubic splines.[31] The term $K^*_{2g,i}(T_o)$ corresponds to the gas−stationary-phase partition coefficient at $T_o$ for the hypothetical *n*-alkane eluting at the same second-dimension temperature, $T$, as solute $i$. $K^*_{2g,i}(T_o)$ values were estimated using a LFER we developed for *n*-alkanes on a BPX50 phase

$$\ln K_{2g,n-\text{alkane}}(T_o) = 0.5440N_c - 1.847 \qquad r^2 = 0.99995, \quad n = 11 \quad (9)$$

where $K_{2g,n-\text{alkane}}(T_o)$ values were determined from isothermal retention times measured on a conventional GC at 120 °C (see Laboratory Analysis) and where $N_c$ is alkane carbon number. The fractional carbon number of the hypothetical *n*-alkane that would elute at $T$ was interpolated from nearby *n*-alkanes. The enthalpy parameter, $a$, was fitted by optimizing the agreement of eq 8 with measured $K_{2g,i}(T_o)$ values (i.e., $K_{2g,i}(T_o)$ values determined from isothermal retention times using a conventional GC at 120 °C) of a set of LACs, LABs, and PAHs. The second dimension retention index, $I_{2,i}$, was found by rescaling $\ln K_{2g,i}(T_o)$ such that $I_{2,n-\text{alkanes}} = 100N_c$ iu, given by

$$I_{2,i} = 183.8 \ln K_{2g,i}(T_o) + 339 \quad (10)$$

The $I_{2,i}$ scale was then compared to the Kováts index ($I'_{2,i}$) obtained from isothermal retention time measurements on a conventional GC at 120 °C.

**Solubility and Vapor Pressure Data.** Experimentally determined vapor pressures,[21,42−44] aqueous solubilities,[21,43,45−48] octanol−water partition coefficients,[21,49] and pure liquid vaporization enthalpies[42,44] of several diesel fuel hydrocarbon compounds at standard conditions (25 °C and 1 atm) were collected from the literature. Air−water partition coefficients were estimated[21] directly from vapor pressure and aqueous solubility data. Care was taken to include data for a wide range of structure types, including *n*-alkanes, LACs, LABs, and PAHs. We verified that the resulting set of equilibrium partitioning data adequately explored a range of sizes and polarities of hydrocarbon compounds found in diesel fuel. Compounds containing O, S, or N, such as thiophenes, carbazoles, furans, or fuel additives, were not considered. Some of the raw vapor pressure and aqueous solubility data were for substances that are solids at 25 °C. Corresponding subcooled liquid vapor pressures ($p_L$) and liquid aqueous solubilities ($C^w_L$) were calculated by accounting for the estimated pure compound free energy of melting, based on melting point and simple molecular structure information.[21,37]

To augment the data set, partitioning property values for a few compounds were estimated using LFERs. The measured aqueous solubilities and vapor pressures of *n*-propyl-, *n*-butyl-, *n*-pentyl-, *n*-hexyl-, and *n*-decyl- LABs were found to follow the LFERs

$$\log C^w_L = -0.668N_c + 2.76 \qquad r^2 = 0.9996, \quad n = 5 \quad (11)$$

$$\log p_L = -0.505N_c + 7.20 \qquad r^2 = 0.99998, \quad n = 5 \quad (12)$$

where $N_c$ is LAB total carbon number. Using eqs 11 and 12, $C^w_L$ and $p_L$ values were estimated for *n*-octylbenzene and *n*-nonylbenzene, since measurement data were not obtained for these compounds. The $C^w_L$ value of *n*-hexylcyclohexane was similarly estimated from a LFER[48] between $C^w_L$ and carbon number for alkylcyclohexanes. This solubility estimate was considered tentative, since the alkylcyclohexanes LFER had been developed from smaller compounds (cyclohexane to *n*-butylcyclohexane).

Aqueous partitioning properties of alkanes larger than undecane were not included in the data set. Although diesel fuels are abundant in *n*-alkanes ranging from $N_c$ = 10 to $N_c$ = 24, most members of this family ($N_c$ > 11) experience folding in aqueous solvent.[50] Consequently, conventional LFERs based on solute size are likely to miscalculate aqueous partitioning properties for large *n*-alkanes. As a rule, the LFER analysis proposed here was not considered reliable for estimating $C^w_L$, $K_{aw}$, and $K_{ow}$ values of hydrocarbon solutes having flexible alkyl chains greater than 11 carbons in length.

## RESULTS AND DISCUSSION

Fifty-seven peaks were identified in the amended diesel fuel mixture, and this set of compounds successfully spanned the two-dimension retention time space of the sample (Figure 1; Table 1). For brevity, we have reported detailed results based on retention data from GC×GC method A, and subsequent discussion refers to the corresponding retention indices unless otherwise specified. To show whether retention indices and physical property estimates are sensitive to differences between the two analytical methods, results from GC×GC method B are also summarized in some sections.


(43) Sherblom, P. M.; Gschwend, P. M.; Eganhouse, R. P. *J. Chem. Eng. Data* **1992**, *37*, 394−399.
(44) CRC *Handbook of Chemistry and Physics*, 77 ed.; CRC Press: Boca Raton, FL, 1997.
(45) Mackay, D.; Shiu, W. Y.; Ma, K. C. *Illustrated Handbook of Physical-Chemical Properties and Environmental Fate for Organic Chemicals. Vol. II, Polynuclear Aromatic Hydrocarbons, Polychlorinated Dioxins, and Dibenzofurans*; Lewis Publishers: Boca Raton, FL, 1992.
(46) Abraham, M. H.; Andonian-Haftvan, J.; Whiting, G. S.; Leo, A.; Taft, R. S. *J. Chem. Soc., Perkin Trans. 2* **1994**, *8*, 1777−1791.
(47) Economou, I. G.; Heidman, J. L.; Tsonopoulos, C.; Wilson, G. M. *AIChE J.* **1997**, *43*, 535−546.
(48) Tsonopoulos, C. *Fluid Phase Equilib.* **2001**, *186*, 185−206.
(49) Abraham, M. H.; Chadha, H. S.; Whiting, G. S.; Mitchell, R. C. *J. Pharm. Sci.* **1994**, *83*, 1085−1100.
(50) Tsonopoulos, C. *Fluid Phase Equilib.* **1999**, *156*, 21−33.

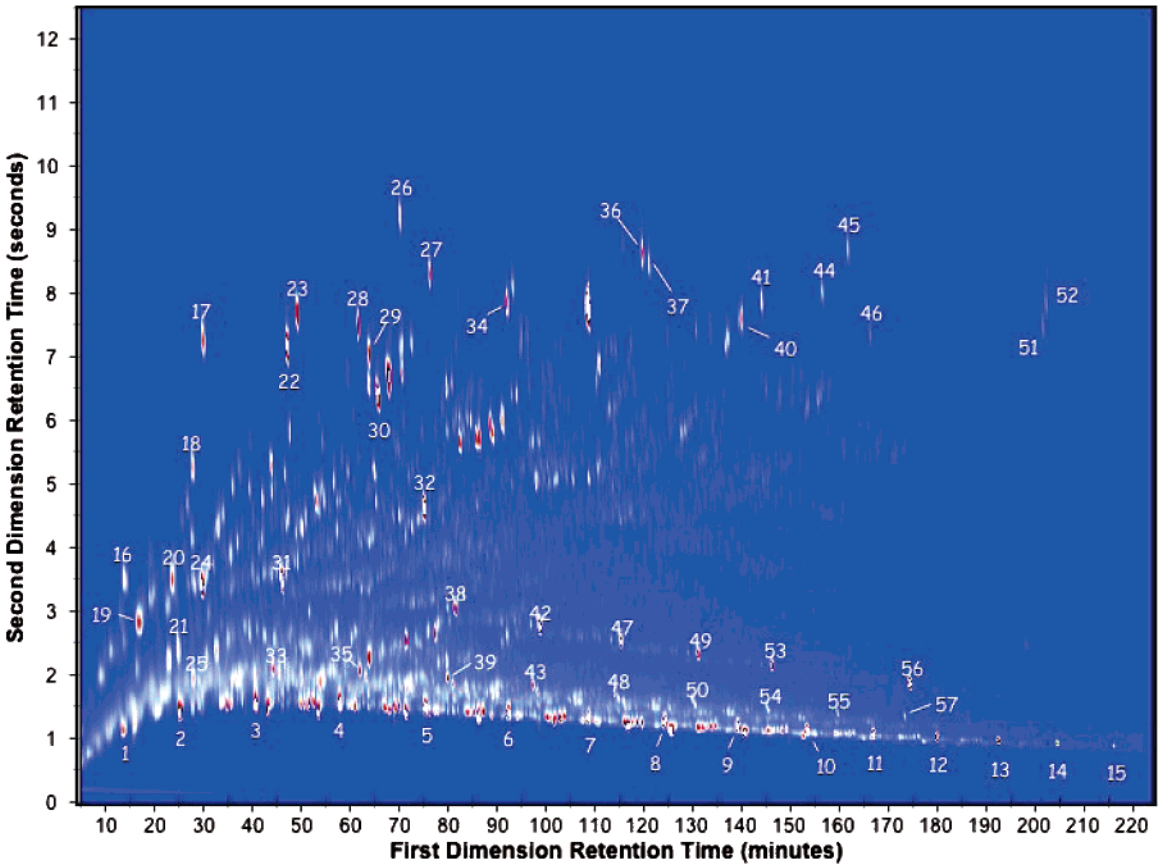


**Figure 1.** GC×GC chromatogram color contour plot of a diesel fuel amended with additional hydrocarbon standards (GC×GC method A). Numbered peaks indicate the compounds used in this study, and these are identified in Table 1. Compounds were separated by volatility in the first dimension. In the second dimension, compounds were further separated by polarity/polarizability; *n*-alkanes eluted early, followed by aliphatic cyclic compounds and then LABs, and finally PAHs eluted last.

**Evaluation of the First-Dimension Retention Index.** The GC×GC first-dimension linear temperature index, $I_{1,i}$, compared favorably with a Kováts index, $I'_{1,i}$ (120 °C). For a set of 10 LACs, 7 LABs, and 9 PAHs ranging from naphthalene to pyrene (Table 1), $I_{1,i}$ values had a root-mean-squared error (rmse) of 20 iu with respect to $I'_{1,i}$. Across all three compound families, $I_{1,i}$ deviations were negative ($I_{1,i} < I'_{1,i}$) for solutes eluting at the lowest first-dimension temperatures. Deviations were incrementally more positive with increasing elution temperature, and the largest members of each series all had positive deviations ($I_{1,i} > I'_{1,i}$). These trends probably occurred because the $\Delta C_p$ of an alkane exceeds that of a less saturated hydrocarbon compound of equivalent volatility.[34,37] Nonetheless, for the temperature range and program conditions under consideration, $I_{1,i}$ did not differ from $I'_{1,i}$ by more than 40 iu for any evaluated solute (Table 1). Briefly, data from GC×GC method B resulted in first-dimension retention indices of similar quality (not shown), having an rmse of 23 iu relative to Kováts values for nonalkane solutes.

**Evaluation of the Second-Dimension Retention Index.** Analysis revealed that eq 8 accurately estimated ln $K_{2g,i}(T_o)$ values from GC×GC second dimension retention time data for representative diesel fuel hydrocarbons. The enthalpy parameter, $a$, was not a sensitive input. Using a training set of 10 LACs, 11 LABs, and 9 PAHs (ranging from naphthalene to pyrene), the optimized value was $a = -1600$ J mol$^{-1}$ and ln $K_{2g,i}(T_o)$ estimates had rmse = 0.076 with respect to values measured isothermally at 120 °C on a conventional GC. Ln $K_{2g,i}(T_o)$ deviations did not show any obvious trends with respect to compound size or family. The corresponding $I_{2,i}$ estimates (eq 10) had rmse = 14 iu with respect to $I'_{2,i}$, the Kováts values. The value for $a$ was not well-determined. Equation 8 discrepancies were only weakly related to $a$, and neglecting the enthalpy parameter altogether (i.e., setting $a = 0$) still resulted in acceptable ln $K_{2g,i}(T_o)$ estimates (rmse = 0.10). This was not considered a disadvantage, since we aimed to formulate retention indices that were not highly sensitive to enthalpy information. Briefly, data obtained using GC×GC method B also gave reasonable second-dimension retention index estimates using eq 10 (not shown); setting $a = -1600$ kJ mol$^{-1}$, nonalkane solutes had a rmse of 21 iu relative to Kováts values.

Despite simplifications about $\Delta H_{2g,i}$, eq 8 conferred some considerable advantages over eq 5 for estimating ln $K_{2g,i}(T_o)$. First, error propagation analysis revealed that the ratio $K_{2g,i}(T)/K^*_{2g,i}(T)$ was about five times less sensitive than $K_{2g,i}(T)$ with respect to perturbations in $\beta_2$ or the measured parameters $t^m_2$ and $t^r_{2,i}$, for the solutes and conditions described here. In other words, the term $K_{2g,i}(T)/K^*_{2g,i}(T)$ in eq 8 was much more reliably estimated from retention data than the analogous term, $K_{2g,i}(T)$, in eq 5; this strategy is similar to the "relative retention"[51] concept. Second, the parameter $a$ in eq 8 supplies information about $\Delta H_{2g,i} - \Delta H^*_{2g,i}$, a difference between two quantities of similar magnitude; consequently the entire temperature correction term in eq 8 contributed only a few percent adjustment to calculated ln

(51) Smith, J. F. *Chem. Ind.* **1960**, 1024−1025.

**Table 1. Identified Solutes in an Amended Diesel Fuel and Their Measured and Calculated Properties, Based on Retention Data from GC×GC Method A**

| no. | compound | $E$ | $V$ | $I_1$ | $I_1'$ | $I_2$ | calc[a] $\ln K_{2g}$ (120 °C) (−)[c] | meas $\ln K_{2g}$ (120 °C) (−)[c] | calc[b] $\log p_L$ (Pa) | meas $\log p_L$ (Pa) | calc[b] $\log C^w_L$ (mol $L^{-1}$) | meas $\log C^w_L$ (mol $L^{-1}$) | calc[b] $\log K_{aw}$ (−)[c] | meas $\log K_{aw}$ (−)[c] | calc[b] $\log K_{ow}$ (−)[c] | meas $\log K_{ow}$ (−)[c] | calc[b] $\Delta H_{vap}$ (kJ $mol^{-1}$) | meas $\Delta H_{vap}$ (kJ $mol^{-1}$) |
|---|---|---|---|---|---|---|---|---|---|---|---|---|---|---|---|---|---|---|
| 1 | decane | 0.000 | 1.518 | 1000 | 1000 | 1000 | 3.59 | 3.59 | 2.17 | 2.24 | −6.38 | −6.42 | 2.21 | 2.27 | 6.22 | 6.25 | 53.9 | 51.38 |
| 2 | undecane | 0.000 | 1.659 | 1100 | 1100 | 1100 | 4.14 | 4.14 | 1.70 | 1.72 | −6.82 | −7.07 | 2.19 | 2.40 | 6.58 | 6.54 | 58.0 | 56.43 |
| 3 | dodecane | 0.000 | 1.799 | 1200 | 1200 | 1200 | 4.68 | 4.68 | 1.24 | 1.19 | na | na[d] | na | na | na | na | 62.2 | 61.51 |
| 4 | tridecane | 0.000 | 1.940 | 1300 | 1300 | 1300 | 5.23 | 5.23 | 0.77 | 0.74 | na | na | na | na | na | na | 66.3 | 66.43 |
| 5 | tetradecane | 0.000 | 2.081 | 1400 | 1400 | 1400 | 5.77 | 5.78 | 0.31 | 0.24 | na | na | na | na | na | na | 70.5 | 71.30 |
| 6 | pentadecane | 0.000 | 2.222 | 1500 | 1500 | 1500 | 6.31 | 6.30 | −0.16 | −0.27 | na | na | na | na | na | na | 74.6 | 76.11 |
| 7 | hexadecane | 0.000 | 2.363 | 1600 | 1600 | 1600 | 6.86 | 6.85 | −0.62 | −0.77 | na | na | na | na | na | na | 78.7 | 81.40 |
| 8 | heptadecane | 0.000 | 2.504 | 1700 | 1700 | 1700 | 7.40 | 7.40 | na | na | na | na | na | na | na | na | 82.9 | 86.02 |
| 9 | octadecane | 0.000 | 2.645 | 1800 | 1800 | 1800 | 7.95 | 7.95 | −1.55 | −1.68 | na | na | na | na | na | na | 87.0 | 84.60 |
| 10 | nonadecane | 0.000 | 2.786 | 1900 | 1900 | 1900 | 8.49 | 8.51 | na | na | na | na | na | na | na | na | na | na |
| 11 | eicosane | 0.000 | 2.927 | 2000 | 2000 | 2000 | 9.03 | 9.05 | −2.48 | −2.35 | na | na | na | na | na | na | 95.3 | 94.00 |
| 12 | heneicosane | 0.000 | 3.068 | 2100 | 2100 | 2100 | 9.58 | 9.58 | na | na | na | na | na | na | na | na | na | na |
| 13 | docosane | 0.000 | 3.208 | 2200 | 2200 | 2200 | 10.12 | 10.12 | −3.40 | −3.59 | na | na | na | na | na | na | 103.6 | 102.50 |
| 14 | tricosane | 0.000 | 3.349 | 2300 | 2300 | 2300 | 10.67 | 10.65 | na | na | na | na | na | na | na | na | na | na |
| 15 | tetracosane | 0.000 | 3.490 | 2400 | 2400 | 2400 | 11.21 | 11.20 | −4.33 | −4.48 | na | na | na | na | na | na | 111.9 | 115.60 |
| 16 | indan | 0.829 | 1.031 | 1002 | na | 1216 | 4.77 | na | 2.16 | 2.30 | −3.54 | −3.03 | −0.71 | −1.06 | 3.77 | 3.33 | na | na |
| 17 | naphthalene | 1.340 | 1.085 | 1132 | 1160 | 1441 | 5.99 | 5.88 | 1.55 | 1.48 | −2.86 | −3.17 | −2.03 | −1.74 | 3.16 | 3.30 | 52.2 | 56.01 |
| 18 | tetralin | na | 1.174 | 1118 | na | 1367 | 5.59 | na | 1.62 | 1.70 | −3.58 | −3.48 | −1.22 | −1.21 | na | na | na | na |
| 19 | *n*-butylbenzene | 0.600 | 1.280 | 1030 | na | 1207 | 4.72 | 4.54 | 2.03 | 2.15 | −4.15 | −3.95 | −0.22 | −0.29 | 4.29 | 4.38 | 51.0 | 51.36 |
| 20 | 1,2,4,5-tetra-methylbenzene | 0.739 | 1.280 | 1087 | na | 1261 | 5.01 | na | 1.76 | 1.54 | −4.46 | −4.15 | −0.18 | −0.70 | 4.54 | 4.10 | na | na |
| 21 | *cis*-decalin | 0.544 | 1.300 | 1097 | na | 1202 | 4.70 | na | 1.72 | 2.00 | −5.40 | −5.26 | 0.75 | 0.87 | na | na | na | na |
| 22 | 2-methyl-naphthalene | 1.304 | 1.226 | 1238 | 1259 | 1526 | 6.45 | 6.41 | 1.06 | 1.05 | −3.60 | −3.65 | −1.77 | −1.69 | 3.78 | 3.86 | na | na |
| 23 | 1-methyl-naphthalene | 1.344 | 1.226 | 1250 | na | 1550 | 6.59 | na | 1.01 | 0.92 | −3.48 | −3.71 | −1.94 | −1.76 | 3.68 | 3.87 | na | na |
| 24 | *n*-pentylbenzene | 0.594 | 1.421 | 1132 | 1144 | 1303 | 5.24 | 5.09 | 1.55 | 1.65 | −4.68 | −4.59 | −0.15 | −0.15 | 4.74 | 4.90 | na | na |
| 25 | *n*-pentyl-cyclohexane | na | 1.550 | 1119 | 1139 | 1187 | 4.61 | 4.60 | 1.61 | 1.68 | −6.00 | −5.97 | 1.26 | 1.26 | na | na | 57.3 | 53.88 |
| 26 | acenaphthylene | 1.750 | 1.216 | 1370 | 1393 | 1704 | 7.42 | 7.49 | 0.45 | 0.55 | −3.56 | −3.99 | −2.43 | −1.85 | 3.73 | 4.00 | na | na |
| 27 | acenaphthene | 1.604 | 1.259 | 1405 | 1426 | 1723 | 7.53 | 7.61 | 0.29 | 0.12 | −3.92 | −3.98 | −2.22 | −2.29 | 4.04 | 3.92 | 63.3 | 62.55 |
| 28 | biphenyl | 1.360 | 1.324 | 1320 | na | 1611 | 6.92 | na | 0.68 | 0.56 | −3.91 | −3.88 | −1.83 | −1.95 | 4.04 | 4.06 | 60.4 | 63.08 |
| 29 | 1-ethylnaphthalene | 1.371 | 1.367 | 1333 | na | 1614 | 6.94 | na | na | na | −4.10 | −4.26 | na | na | 4.20 | 4.39 | na | na |
| 30 | 2,6-dimethyl-naphthalene | 1.329 | 1.367 | 1343 | na | 1608 | 6.90 | na | na | na | −4.35 | −4.12 | na | na | 4.41 | 4.31 | na | na |
| 31 | *n*-hexylbenzene | 0.591 | 1.562 | 1232 | 1233 | 1388 | 5.70 | 5.64 | 1.09 | 1.13 | −5.32 | −5.20 | 0.03 | −0.06 | 5.27 | 5.52 | na | na |
| 32 | hexamethyl-benzene | na | 1.562 | 1398 | na | 1610 | 6.91 | na | 0.32 | 0.09 | −5.30 | −4.95 | −0.77 | −1.35 | 5.23 | 4.75 | na | na |
| 33 | *n*-hexylcyclo-hexane | na | 1.691 | 1221 | 1228 | 1281 | 5.12 | 5.15 | na | na | −6.54 | −6.52 | na | na | na | na | na | na |
| 34 | fluorene | 1.588 | 1.357 | 1497 | 1512 | 1820 | 8.05 | 8.13 | −0.14 | −0.21 | −4.27 | −4.13 | −2.30 | −2.47 | 4.33 | 4.18 | 67.0 | 67.43 |
| 35 | *n*-heptylcyclo-hexane | na | 1.832 | 1322 | 1316 | 1375 | 5.63 | 5.69 | na | na | na | na | na | na | na | na | na | na |
| 36 | phenanthrene | 2.055 | 1.454 | 1670 | 1675 | 2040 | 9.25 | 9.34 | −0.94 | −0.98 | −4.40 | −4.52 | −2.98 | −2.85 | 4.41 | 4.46 | 73.1 | 74.40 |
| 37 | anthracene | 2.290 | 1.454 | 1679 | 1683 | 2046 | 9.28 | 9.30 | −0.99 | −1.49 | −4.49 | −5.08 | −2.93 | −2.80 | 4.49 | 4.45 | na | na |
| 38 | *n*-octylbenzene | 0.579 | 1.844 | 1435 | 1419 | 1568 | 6.69 | 6.75 | 0.14 | 0.13 | −6.52 | −6.59 | 0.30 | 0.33 | 6.28 | 6.34 | na | na |
| 39 | *n*-octylcyclo-hexane | na | 1.973 | 1426 | 1417 | 1475 | 6.18 | 6.23 | na | na | na | na | na | na | na | na | na | na |
| 40 | 1-methyl-phenanthrene | 2.055 | 1.595 | 1804 | na | 2167 | 9.94 | na | na | na | −5.08 | −4.93 | na | na | 4.98 | 5.08 | na | na |
| 41 | 9-methyl-anthracene | 2.290 | 1.595 | 1833 | na | 2204 | 10.15 | na | na | na | −5.10 | −5.37 | na | na | 4.99 | 5.07 | na | na |
| 42 | *n*-nonylbenzene | na | 1.984 | 1539 | 1519 | 1666 | 7.22 | 7.29 | −0.33 | −0.38 | −7.04 | −7.26 | 0.35 | 0.49 | na | na | na | na |
| 43 | *n*-nonylcyclo-hexane | na | 2.114 | 1530 | 1517 | 1579 | 6.74 | 6.78 | na | na | na | na | na | na | na | na | na | na |
| 44 | fluoranthene | 2.377 | 1.585 | 1921 | 1901 | 2310 | 10.72 | 10.72 | −2.11 | −2.15 | −5.24 | −5.20 | −3.30 | −3.34 | 5.10 | 5.16 | 83.0 | 75.15 |
| 45 | pyrene | 2.808 | 1.585 | 1959 | 1935 | 2375 | 11.07 | 11.00 | −2.29 | −2.19 | −5.06 | −5.26 | −3.67 | −3.32 | 4.94 | 4.88 | 84.0 | 86.80 |
| 46 | 9,10-dimethyl-anthracene | 2.290 | 1.736 | 1994 | na | 2378 | 11.09 | na | na | na | −5.63 | −5.33 | na | na | 5.42 | 5.69 | na | na |
| 47 | *n*-decylbenzene | 0.579 | 2.125 | 1641 | 1619 | 1764 | 7.75 | 7.85 | −0.81 | −0.88 | −7.56 | −7.94 | 0.40 | 0.67 | 7.15 | 7.40 | 77.6 | 79.10 |
| 48 | *n*-decylcyclo-hexane | na | 2.254 | 1633 | 1617 | 1682 | 7.30 | 7.33 | −0.77 | −0.87 | na | na | na | na | na | na | 79.0 | 79.05 |
| 49 | *n*-undecylbenzene | 0.579 | 2.266 | 1745 | na | 1865 | 8.30 | 8.35 | −1.29 | −0.79 | na | na | na | na | na | na | na | na |
| 50 | *n*-undecyl-cyclohexane | na | 2.395 | 1737 | 1717 | 1788 | 7.88 | 7.88 | na | na | na | na | na | na | na | na | na | na |
| 51 | benz[*a*]anthracene | 2.992 | 1.823 | 2275 | na | 2696 | 12.82 | na | −3.75 | −3.26 | −6.37 | −5.98 | −3.81 | −3.67 | 6.03 | 5.79 | na | na |
| 52 | chrysene | 3.027 | 1.823 | 2280 | na | 2712 | 12.91 | 12.73 | −3.78 | −4.18 | −6.26 | −6.01 | −3.96 | −4.56 | 5.93 | 5.73 | 96.9 | 96.85 |
| 53 | *n*-dodecylbenzene | 0.579 | 2.407 | 1848 | 1820 | 1965 | 8.84 | 8.95 | −1.77 | −1.19 | na | na | na | na | na | na | na | na |
| 54 | *n*-dodecyl-cyclohexane | na | 2.536 | 1839 | 1818 | 1890 | 8.44 | 8.43 | na | na | na | na | na | na | na | na | na | na |
| 55 | *n*-tridecylcyclo-hexane | na | 2.677 | 1944 | 1918 | 1994 | 9.00 | 8.98 | na | na | na | na | na | na | na | na | na | na |
| 56 | *n*-tetradecyl-benzene | na | 2.689 | 2056 | 2018 | 2180 | 10.01 | 10.04 | −2.74 | −2.51 | na | na | na | na | na | na | 94.8 | 91.70 |
| 57 | *n*-tetradecyl-cyclohexane | na | 2.818 | 2048 | 2016 | 2099 | 9.57 | 9.52 | na | na | na | na | na | na | na | na | na | na |

[a] Calculated using eq 8. [b] Calculated using eq 2. [c] Dimensionless partition coefficients are given in units of (mol $L^{-1}$)(mol $L^{-1}$)$^{-1}$. [d] na refers to entries where data were not available or could not be compared to available data.

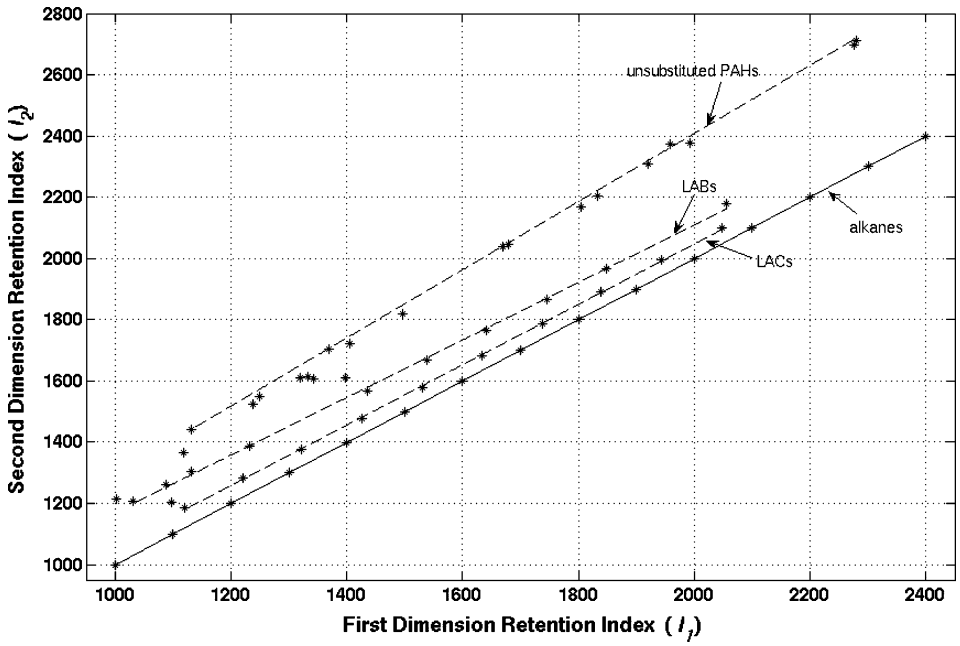


**Figure 2.** Calculated retention indices for 57 diesel fuel solutes, using retention data from GC×GC method A. The *n*-alkane series was defined from $I_{1,i} = I_{2,i} = 1000$ iu (decane) to $I_{1,i} = I_{2,i} = 2400$ iu (tetracosane), as depicted by the contiguous solid line (—). Calculated $I_{2,i}$ values of LACs, LABs, and PAHs departed farther from the *n*-alkane reference line with increasing solute polarity, as shown by the dashed lines (- - -) corresponding to eqs 13−15, respectively.

$K_{2g,i}(T_o)$ values. In previous work on GC×GC, estimating second-dimension retention indices was burdened by the difficulty of accurate temperature corrections.[28] Additionally, in typical GC×GC samples, we anticipate that second-dimension retention index data correlate with first-dimension retention index data (Figure 2). For the two retention indices to be independently useful, it is critical that they are as distinguishable as possible for a given sample of interest. In the current work, the expected correlation between the first and second retention indices was turned to an advantage. The *n*-alkane series falls on a line in the first-dimension versus second-dimension retention index space (Figure 2); the second-dimension retention indices of all solutes were thus essentially estimated as departures from this reference line.

Hydrocarbon compound families were internally consistent in the GC×GC retention index space. We expected any homologous series to form a straight line in a plot of the first-dimension versus second-dimension retention index space. Accordingly, via linear regressions we found

$$I_{2,\mathrm{LACs}} = 0.986 I_{1,\mathrm{LACs}} + 75 \qquad r^2 = 0.9998, \quad n = 10 \qquad (13)$$

$$I_{2,\mathrm{LABs}} = 0.939 I_{1,\mathrm{LABs}} + 231 \qquad r^2 = 0.9991, \quad n = 9 \qquad (14)$$

$$I_{2,\mathrm{PAHs}} = 1.113 I_{1,\mathrm{PAHs}} + 182 \qquad r^2 = 0.9998, \quad n = 5 \qquad (15)$$

where the PAH series (eq 15) included naphthalene, acenaphthylene, phenanthrene, pyrene, and chrysene. These results confirmed that the first-dimension versus second-dimension retention index space was internally precise over wide ranges of both solute size ($N_c = 10$ to $N_c = 24$) and solute polarity (alkanes to PAHs).

**Solute Size and Polarity/Polarizability Information in the GC×GC Retention Index Space.** Multiple linear regressions showed that the first- and second-dimension retention indices were accurately explained by the solute size[24] (*V*) and excess polarizability[52] (*E*) descriptors of Abraham and co-workers. *V* is a group contributable solute molecular volume.[24] *E* is defined as the measured liquid or gas molar refraction of a solute at 20 °C minus that of a hypothetical alkane of identical volume.[26] We found

$$I_{1,i} = 331.2E + 680.1V \qquad r^2 = 0.995, \quad n = 43 \qquad (16)$$

$$I_{2,i} = 1.008 I_{1,i} + 166.3E \qquad r^2 = 0.996, \quad n = 43 \qquad (17)$$

where regression intercepts were not statistically significant for either eq 16 or 17. It is worth noting that many aromatic hydrocarbon compounds in diesel fuel also have nonnegligible electrostatic (*S*) and hydrogen-bond acceptor (*B*) solvation descriptors;[52] one may reasonably suspect that these effects contribute importantly to solute interactions with polar solvents such as water. We found that *S* and *B* both correlated strongly with *E* ($r^2 = 0.985$ and $r^2 = 0.91$, respectively) across the compound set. Therefore we concluded that the information contained in *S* and *B* was captured by *E* in fits of eqs 16 and 17, for hydrocarbon solutes. Equations 16 and 17 show that the first-dimension and second-dimension retention indices contained different amounts of solute size and solute polarity/polarizability information. This explains why the first- and second-dimension stationary phases separated the hydrocarbon mixture effectively: the sample explored primarily only two dimensions of information about solute−stationary-phase molecular interactions.

**Estimating Partitioning Properties for Diesel Fuel Hydrocarbons.** Using retention data from GC×GC method A, resulting retention indices successfully explained several partitioning properties of the diesel fuel hydrocarbon solute set (Table

(52) Abraham, M. H. *J. Chromatogr.* **1993**, *644*, 95−139.

**Table 2. Regression Statistics[a] for Hydrocarbon Solute Partitioning Property Estimates Using Eq 2**

| solute property | GC×GC method | $a_{xy}$ | $b_{xy}$ | $c_{xy}$ | $r^2$ | std dev | n |
|---|---|---|---|---|---|---|---|
| log $p_L$ (Pa) | A | −0.00464 ± 0.0001 | | 6.81 ± 0.14 | 0.99 | 0.21 | 40 |
| log $p_L$ (Pa) | B | −0.00458 ± 0.0001 | | 6.74 ± 0.15 | 0.99 | 0.22 | 39 |
| log $C_L^w$ (mol $L^{-1}$) | A | −0.0177 ± 0.0007 | 0.0133 ± 0.0005 | −2.00 ± 0.22 | 0.96 | 0.26 | 33 |
| log $C_L^w$ (mol $L^{-1}$) | B | −0.0175 ± 0.0007 | 0.0134 ± 0.0006 | −2.47 ± 0.19 | 0.96 | 0.25 | 32 |
| log $K_{aw}$ (−)[b] | A | 0.0134 ± 0.0007 | −0.0136 ± 0.0005 | −2.43 ± 0.28 | 0.98 | 0.27 | 27 |
| log $K_{aw}$ (−)[b] | B | 0.0132 ± 0.0007 | −0.0137 ± 0.0005 | −2.78 ± 0.25 | 0.98 | 0.27 | 26 |
| log $K_{ow}$ (−)[b] | A | 0.0151 ± 0.0006 | −0.0115 ± 0.0004 | −2.58 ± 0.20 | 0.96 | 0.21 | 28 |
| log $K_{ow}$ (−)[b] | B | 0.0147 ± 0.0008 | −0.0114 ± 0.0006 | −3.00 ± 0.20 | 0.95 | 0.23 | 27 |
| $\Delta H_{vap}$ (kJ $mol^{-1}$) | A | 0.065 ± 0.004 | −0.023 ± 0.004 | 12.4 ± 2.3 | 0.98 | 2.7 | 25 |
| $\Delta H_{vap}$ (kJ $mol^{-1}$) | B | 0.066 ± 0.005 | −0.025 ± 0.005 | 13.3 ± 2.4 | 0.97 | 2.7 | 25 |

[a] Multiple linear regressions were performed using singular value decomposition.[55] Reported uncertainties for $a_{xy}$, $b_{xy}$, and $c_{xy}$ correspond to ± one standard error of the fitted values, estimated using the bootstrap method[56] with 1000 synthetic samples. [b] Dimensionless partition coefficients are given in implicit units of (mol $L^{-1}$)(mol $L^{-1}$)$^{-1}$.

1), via multiple linear regressions of eq 2 (Table 2). Regression-calculated vapor pressures, aqueous solubilities, air−water partition coefficients, and octanol−water partition coefficients were typically within a factor of 2 of measured values. $\Delta H_{vap}$ was also accurately fitted using eq 2, usually within 3 kJ $mol^{-1}$ of reported measurements. By comparison, retention indices derived from GC×GC method B gave similar regression coefficients and nearly identical fit statistics when applied to eq 2 (Table 2). This shows that eq 2 was reliable over the range of GC×GC temperature programs and other instrument settings explored by method A and method B.

Equation 2 fits of the aqueous partitioning properties required both GC×GC retention indices. Estimates of log $C_L^w$, log $K_{aw}$, and log $K_{ow}$ using only either $I_{2,i}$ or $I_{1,i}$ as a regression variable resulted in significantly poorer fits ($r^2 \leq 0.10$ for log $C_L^w$, $r^2 \leq 0.70$ for log $K_{aw}$, and $r^2 \leq 0.12$ for log $K_{ow}$). Consistent with our prior expectations, both solute size and polarity/polarizability information were needed to accurately describe solute−solvent interactions for hydrocarbon solutes in aqueous systems. Consequently it is clear that a conventional one-dimensional GC retention index could not have predicted aqueous partitioning properties (i.e., via eq 1) for the range of hydrocarbon compound types considered here. Liquid vapor pressure estimates required only the first-dimension retention index; the fitted coefficient to $I_{2,i}$ was not statistically significant.

Data quality may have partly limited the success of eq 2 regressions. Particularly for sparingly soluble compounds, aqueous partitioning property measurements may reasonably err by a factor of 2,[21] consistent with the magnitude of typical eq 2 deviations for $C_L^w$, $K_{aw}$, and $K_{ow}$ (Table 1). Additionally, estimated log $p_L$ and log $C_L^w$ data for compounds with high melting temperatures[21] (e.g., anthracene, $T_{melt}$ = 217.5 °C; chrysene, $T_{melt}$ = 255 °C; 9,10-dimethylanthracene, $T_{melt}$ = 182 °C; hexamethylbenzene, $T_{melt}$ = 166 °C) might have erred by 0.1−0.2 due to melting energy corrections, based on our analysis of propagated uncertainty in the entropy of melting estimates.[21] Notably, these compounds had some of the larger eq 2 deviations (~0.3−0.5) for the properties that involved melting energy corrections, log $p_L$ and log $C_L^w$. Finally, we note that anthracene is among the largest deviations for both log $p_L$ and log $C_L^w$ regressions. In addition to melting energy uncertainty, these apparent deviations may result from the difficulty of accurate laboratory measurements, since anthracene is photoreactive.[53]

## CONCLUSIONS AND IMPLICATIONS

Using alkanes as reference solutes, GC×GC retention indices were accurately estimated for several hydrocarbon solutes found in diesel fuel. The new method is mathematically straightforward and did not require any special instrumentation protocols such as multiple injections or unusual temperature programming. A single-injection run with dual linear temperature ramp programs was employed; this is a very typical GC×GC analysis. Resulting retention index estimates were robust. The second-dimension retention index estimate appears much less sensitive to uncertainties in measured retention parameters and enthalpy information than a retention index based on direct temperature corrections (eq 5). Retention index estimates were very comparable using two widely different temperature programs (method A versus method B). Additionally, since fuel components displayed independent (i.e., infinitely dilute) retention behavior, peaks that might represent two or more coeluting solutes would still be assigned accurate retention indices. Finally, sample-dimension information was effectively analyzed from GC×GC retention index estimates in terms of the molecular descriptors $E$ and $V$. It is important to also notice some limitations: first, the linear temperature index is slightly dependent on the GC×GC flow and temperature regime. Second, the simple approximation for $\Delta H_{2g,i}$ (eq 7) was not evaluated for solutes other than hydrocarbons. It would be interesting to compare the second-dimension retention index estimated using eq 8 to the approaches proposed by Western and Marriott.[28] However, since these authors have published few actual predicted values using their method, meaningful comparisons are currently difficult. In future work, eq 8 could be evaluated for other solutes: for more polar samples, the second-dimension retention index might be extrapolated from a more appropriate reference series than alkanes. The simplifications employed here allowed retention index estimates using very limited information about the structures of sample mixture components. In future work, the approximations we have made for $\Delta H_{2g,i}$ might be improved using solute structure information. In cases where the appropriate solute

(53) Gschwend, P. M.; Hites, R. A. *Geochim. Cosmochim. Acta* **1981**, *45*, 2359−2367.

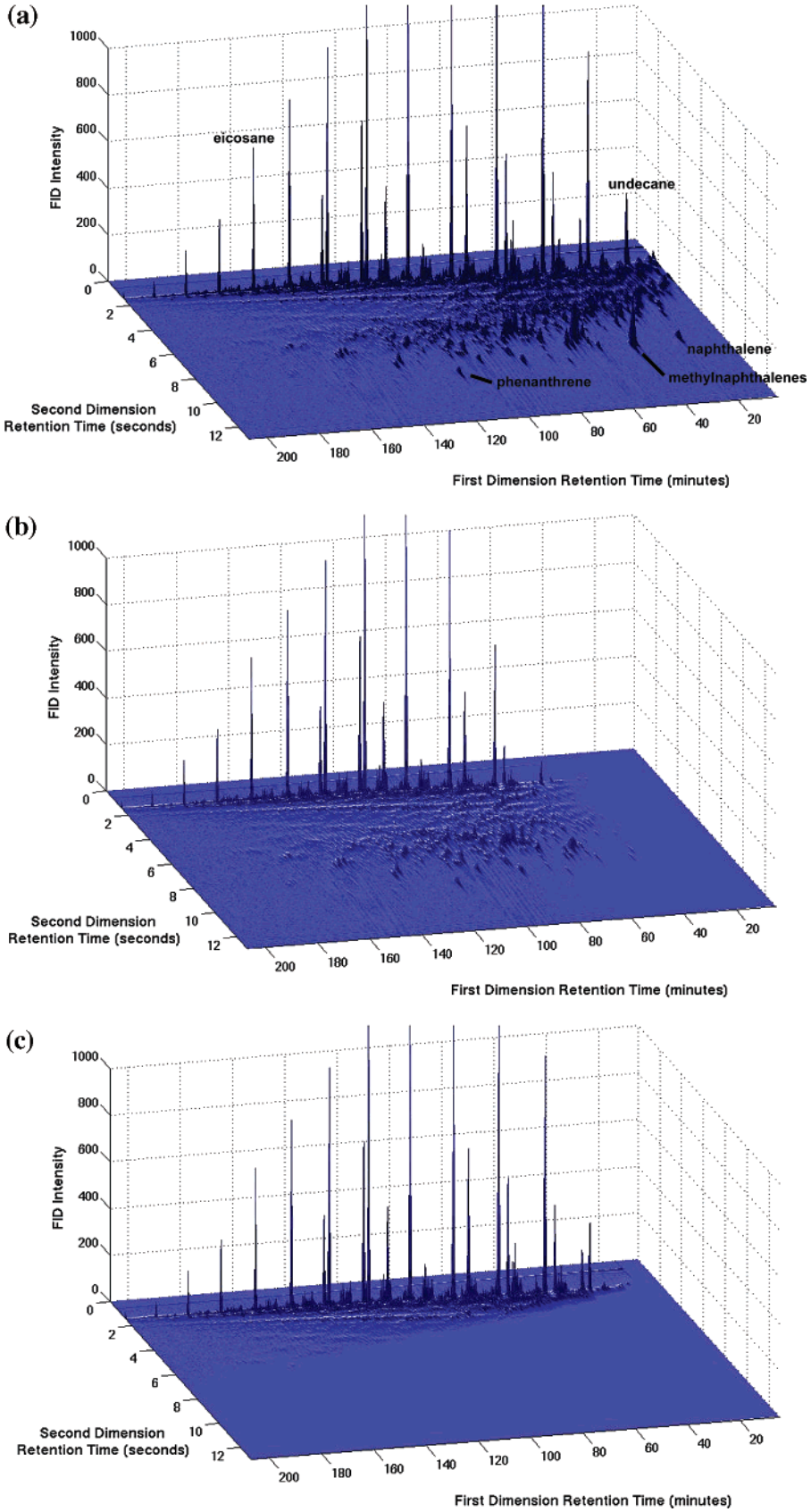


**Figure 3.** GC×GC chromatogram mountain plots of original *Bouchard 65* fuel, before and after simulated weathering. (a) GC×GC chromatogram of the original, unamended *Bouchard 65* diesel fuel sample using GC×GC method A. A mountain plot is shown to emphasize the relative abundances of resolved mixture components; a few compounds are labeled to help orient the reader. (b) Simulated GC×GC chromatogram of neat *Bouchard 65* fuel after 50% of the mass was evaporated. (c) Simulated GC×GC chromatogram of neat *Bouchard 65* fuel after 50% of the mass was aqueously dissolved.

data are available, models[54] might be used to convert the first-dimension linear temperature index into a better estimate of the Kováts index, thereby improving its reliability and interpretability. Finally, in future GC×GC applications of more complex samples, hydrogen bonding and electrostatic descriptors (*A*, *B*, *S*) may be necessary to interpret retention indices and thus guide estimates of sample separability.

We estimated several useful partitioning properties of diesel fuel solutes from GC×GC retention indices; this was not possible using a conventional one-dimensional GC retention index. We do not recommend eq 2 for estimating hydrocarbon partitioning properties in general, since more accurate methods[43] have been developed for this task. Additionally, since linear temperature index deviations from the Kováts scale are systematic[35,54] with respect to compound size and family, eq 2 regressions inevitably incorporated some of this information. Use of a different temperature ramping rate (method B) resulted in slightly shifted linear retention index values, and this in turn affected the best-fit regression coefficients of eq 2 to a small extent. Therefore the eq 2 regression coefficients reported in this work (Table 2) may not be optimal for other temperature programs and GC×GC conditions. However, these results also demonstrate that eq 2 fits are relatively insensitive to the temperature program settings, suggesting that the success of eq 2 was not an idiosyncratic result of the particular GC×GC analysis settings we chose. Hence we might reasonably expect to achieve similarly good fits of partitioning properties of hydrocarbons using other GC×GC programs.

Environmental researchers could use eq 2 to incisively analyze phase-transfer processes affecting complex mixtures. Each point on the GC×GC chromatogram has a unique $I_{1,i}$ and $I_{2,i}$ value; consequently, solute partitioning property estimates were mapped to the entire two-dimensional retention time space. In other words, as a result of the powerful relationships developed from eq 2, most of the chromatogram peaks—including coeluting solutes—do not have to be assigned exact compound structures (assuming they are hydrocarbons) in order to model effects of phase-transfer processes on the complete mixture. For example, we used the results from this study to illustrate simulated environmental processes that could act on the *Bouchard 65* fuel. We assumed that the rates of volatilization and dissolution of hydrocarbons from the diesel fuel were directly controlled by solute $p_L$ and $C_L^w$ values, respectively. Shown in Figure 3 are the following: a GC×GC chromatogram of original fuel (a) and simulated chromatograms of the fuel after 50% mass removal due to either evaporation (b) or aqueous dissolution (c). It is visually apparent that these anticipated signatures are distinct. In forthcoming work, the simulated effects of water washing and evaporation on neat petroleum liquids will be compared to GC×GC data of the residual weathered mixtures found at contaminated field sites. Phase transfer to air and water might be distinguished from other environmental processes that selectively remove constituents from hydrocarbon mixtures, such as biodegradation and phototransformation. As a result, the increased resolution and physical property estimates afforded by GC×GC may significantly advance our understanding of processes that act on petroleum hydrocarbons in the environment.

(54) White, C. M.; Hackett, J.; Anderson, R. R.; Kail, S.; Spock, P. S. *J. High Resolut. Chromatogr.* **1992**, *15*, 105−120.
(55) Press, W. H.; Teukolsky, S. A.; Vetterling, W. T.; Flannery, B. P. *Numerical Recipes in C: The Art of Scientific Computing*; Cambridge University Press: Cambridge, 1993.
(56) Efron, B.; Tibshirani, R. *Stat. Sci.* **1986**, *1*, 54−77.

## ACKNOWLEDGMENT

We thank Ms. Emily E. Peacock (WHOI) and Drs. Philip M. Gschwend (MIT), Richard B. Gaines (USCGA), Glenn S. Frysinger (USCGA), Jean K. Whelan (WHOI), Christine M. Roth (Harvard), Federico M. san Martini (MIT), Kai Udert (MIT), and Thomas B. Hofstetter (EAWAG) for their assistance in this project. This work was supported by funds from the Environmental Protection Agency (R-830393), an Office of Naval Research Young Investigator Award (N00014-04-01-0029), the National Science Foundation (IIS-0430835), and the Lovell Foundation.

Received for review June 14, 2005. Accepted September 3, 2005.

AC051051N